

Test of a Large Energy Acceptance NS-FFAG Arc at the ATF

PI: Stephen Brooks

v2, 2016-Sep-28

Collaborators: Dejan Trbojevic, George Mahler, Mikhail Fedurin (maybe more)

1. Introduction and Goals

The tuneable-energy electron beam available at ATF can be used to demonstrate a type of beam transport called a linear-field “non-scaling FFAG”, or NS-FFAG, where “FFAG” stands for fixed-field alternating-gradient accelerator. This type of lattice can transmit a wide range of particle momenta without having to change the magnet field strengths (as is done in synchrotrons), so the different momentum beams can be transported simultaneously, on slightly different orbits within the same magnets. Additionally, the linear-field version used here can accomplish this with only combinations of quadrupole and dipole.

Permanent magnets already bought for CBETA R&D can be used to produce such a beamline approximately 1.5m long with a 40 degree bend, which is capable of transmitting a factor of 4 in energy: 20-80MeV. This can be installed on a beam port at ATF with a screen at the end to record the output beam centroid position as a function of input position, angle and energy, which gives information about the optics and phase advance through the beamline.

1.1. FFAG Electron Transport for eRHIC

A major motivation for demonstrating a NS-FFAG beamline with a large momentum acceptance is that such a beamline reduces the cost of electron transport in eRHIC, where many different energy passes have to travel around the RHIC tunnel back to the energy-recovery linac. In various designs explored since 2013, 12-16 passes can be combined into just two FFAG loops, or alternatively 8 passes can be combined into one FFAG and one conventional loop.

Currently, the baseline eRHIC design is forbidden from containing any technology that is not demonstrated to some level of confidence, so that at any point the total risk in the design will remain manageable. This means it does not currently use FFAG return loops, giving a large number of separate conventional loops, which puts limits on the total number of passes, requiring a longer linac to reach a given energy. However, an early demonstration of NS-FFAG arc optics could then avoid the eRHIC design being driven down an unnecessarily low-performance or high-cost path.

1.2. Relationship to CBETA

The CBETA machine being built at Cornell is another risk-reducing technology demonstration for eRHIC, which includes not only FFAG return loops, but a multi-pass superconducting ERL, splitter lines and FFAG magnet corrector coils as well. It will be an integrated test of many new technologies proposed for eRHIC, so if successful it will provide a high level of confidence in this approach. However, it is currently scheduled for full operation in late 2019, which is quite a long time to wait for permission to use FFAGs in the eRHIC design.

This ATF NS-FFAG beamline has much smaller scope but will be able to tell early on (2017) if there is a fundamental problem with either the non-scaling FFAG lattice or its implementation using permanent magnets. Either of these would be very important to know about for CBETA and in turn eRHIC.

1.3. Technology for Hadron Therapy Gantry

The ability of FFAGs to transmit multiple energies without magnet changes makes them an interesting possibility for hadron therapy gantries, which rapidly scan the particle energy in order to irradiate different depths inside the patient. As shown in the table below, the particle momentum required for proton therapy is larger than either ATF or CBETA, but is still feasible on a 5 metre radius bend. This gives a gantry that is larger in radius than a superconducting or electromagnet option but it is much lighter, with under 1 tonne of magnet material. The magnets required are longer but otherwise not very different from those to be demonstrated in the ATF FFAG.

Parameter	ATF FFAG	Gantry	Units
Particle species	Electron	Proton	
Kinetic energy range	20–80	50–250	MeV
Momentum range	20.5–80.5	310.4–729.1	MeV/c
Cell Length	0.251751	0.537588	m
Cell Angle	6.666...	6.16030	degrees
R = avg. radius of curvature	2.16364	5	m
Max orbit excursion (in QF)	19.83	17.01	mm (from circle radius R)
Magnet bore radius (QF, BD)	37.20, 30.70	27.61, 27.61	mm (without shims)
Tune range per cell	0.032–0.410	0.031–0.379	cycles
Drift lengths	67.55, 64.90	50, 50	mm
Magnet lengths (QF, BD)	57.44, 61.86	223.42, 214.16	mm
Magnet material grade	N35SH	N48H	
Effective B_r	1.194	1.4	T
Magnet max radius	62.45	78.58	mm
Magnet cross-section (QF, BD)	75.35, 46.71	100.91, 96.83	cm ²
Magnet mass per cell	5.486	32.89	kg
Magnet mass per 180°	148.1	961.1	kg

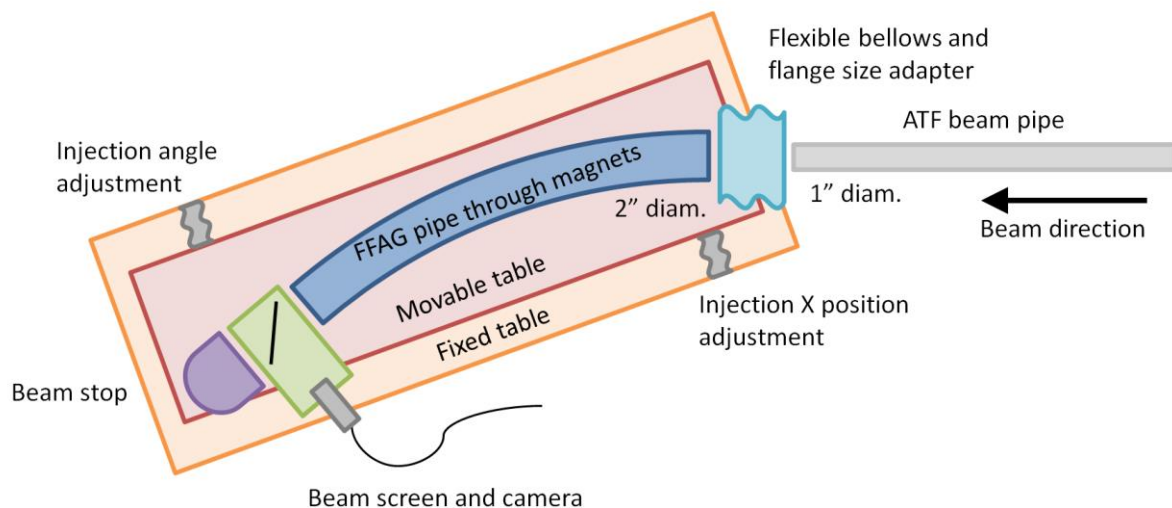
2. Proposed Non-Scaling FFAG Beamline

The overall parameters and dimensions of the beamline are given in the table below.

Parameter	Value	Units
Particle species	Electron	
Energy range	20-80	MeV
Cell Length	0.251751	m
Cell Angle	6.666...	degrees (54 per turn)
R = avg. radius of curvature	2.16364	m
Max orbit excursion	19.83	mm (from circle radius R)
Tune range per cell	$Q_{y,80} = 0.032, Q_{x,20} = 0.410$	cycles
Cell lattice	halfD2, QF, D1, BD, halfD2	
Drift lengths	D1 = 67.55, D2 = 64.90	mm
Number of cells	6	
Total length	1.51051	m
Total angle	40	degrees

2.1. Outline of Main Components

A schematic of the parts to be assembled for this experiment is shown below.



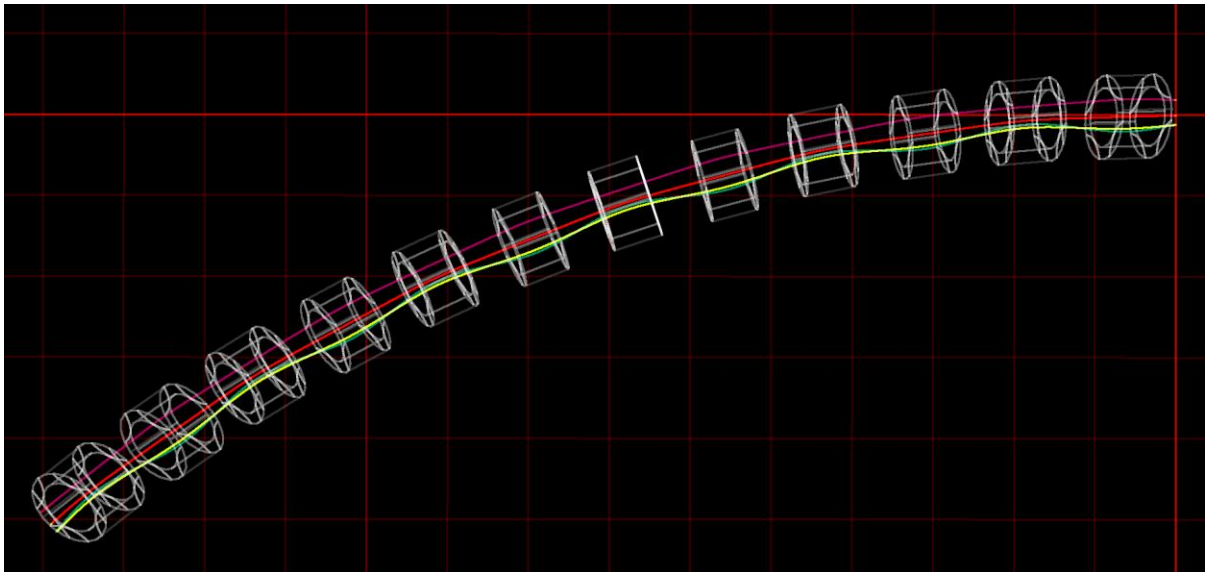
The ATF beam has some position/angle scanning capability but it comes from a smaller aperture pipe than the FFAG uses and thus cannot cover the full range of entrance positions and angles. The experiment provides additional adjustment of the injection position and angle by putting the entire beamline on a movable table (fortunately the beamline is very compact). This will only need to be adjusted per beam energy setting and can remain fixed for injection position/angle scans.

As the entrance to the FFAG may move by up to ~2cm laterally relative to ATF, there is a flexible bellows joining the two, which may also be the adaptor from the smaller to larger flange size.

The end of the FFAG is attached directly to a beam screen diagnostic, which is attached directly to a beam stop. More information on the FFAG and diagnostic are given in the subsections that follow.

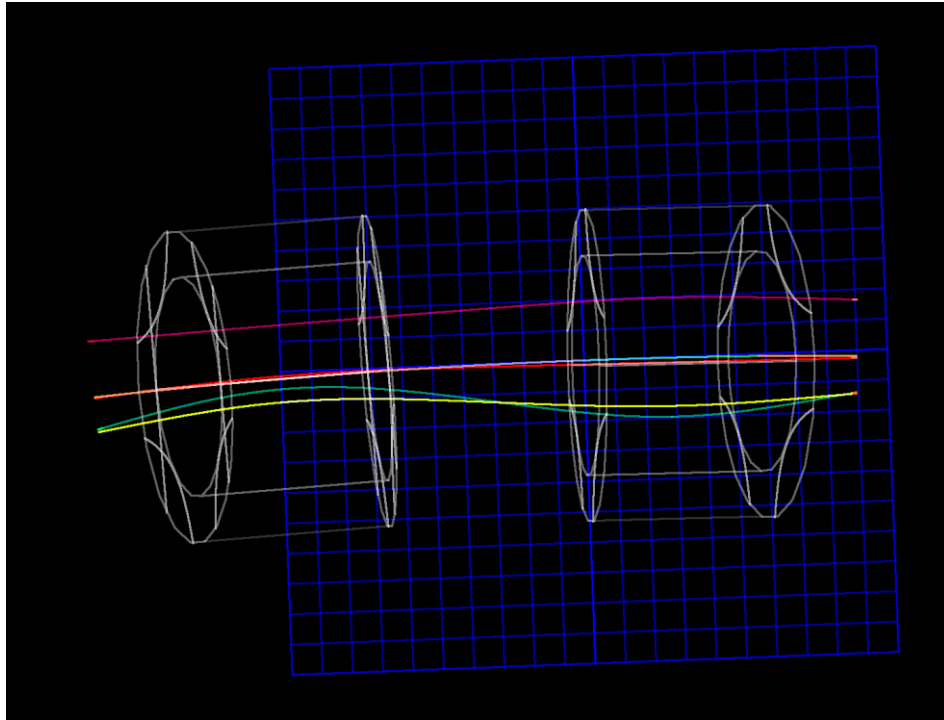
2.2. FFAG Beam Optics

The figure below shows the layout of the 6-cell beamline (12 magnets in total) with 20, 40, 60, 80MeV orbits to scale. The background grid is 10cm spacing, so the beamline ends at (Z,X) = (1.39076,-0.50620) metres.



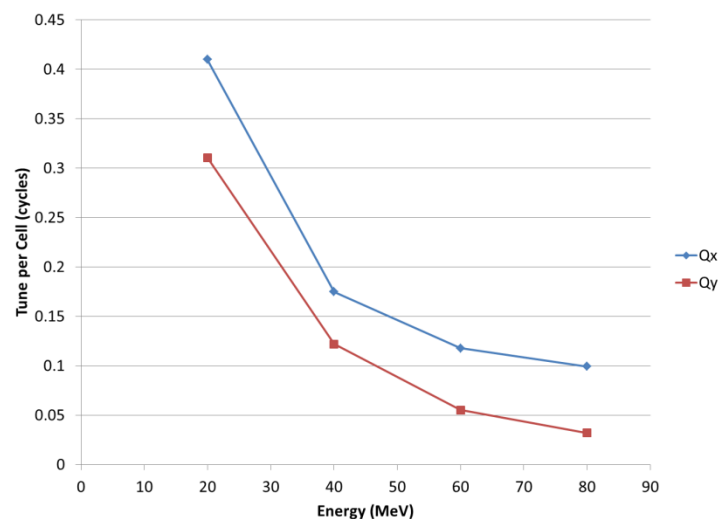
This simulation was done in Muon1 with a soft-edged Maxwellian field model. In studies for the CBETA FFAG arc, good agreement was obtained between orbits using OPERA-3D fieldmaps and orbits using Muon1's model (<1mm difference), although this check will also be redone for this lattice when OPERA-3D fieldmaps for the magnets have been calculated.

The orbits through a single cell for 20, 40, 60, 80MeV are shown below with QF on the right and BD on the left (beams direction is to the left). The grid is 1cm squares.



The orbits in QF are arranged in order of increasing energy from inside to outside, so if the tight $\sim 4\text{mm}$ gap between the beam centres and the inside of the vacuum chamber is a problem, it will be the extreme ends of the 20-80MeV energy range that are lost, with intermediate energies still transmitted. Notably the 60MeV orbit stays very close to the circle of the vacuum chamber centre, which is also shown in the figure.

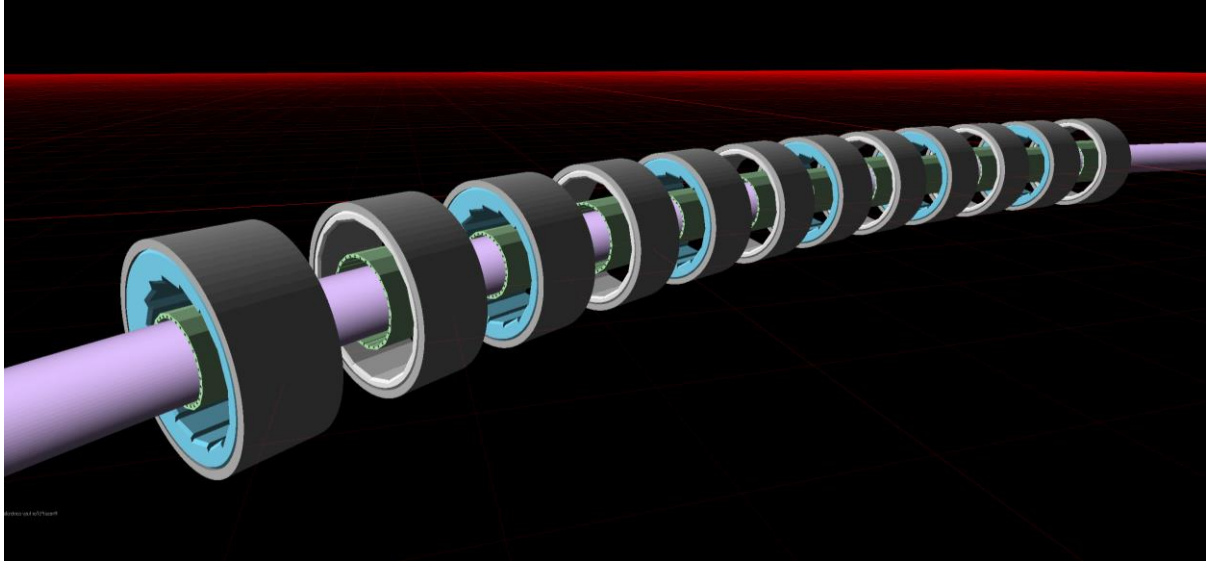
The graph below shows the phase advance per cell for each of these four energies. This wide range brackets the phase advances proposed for most future NS-FFAG machines.



The more rapid variation of tunes near the low energy end may mean it would be better to have closer energy steps there.

2.3. FFAG Construction

The figure below shows how a toroidal vacuum pipe (purple) fits through the shim holders (green) that are placed inside each magnet (the permanent magnet blocks are not shown), which are in turn inside the 3D printed mould (BD blue and QF white) and outer aluminium support (grey).



In order to fit the 4x energy range through the existing magnets, the lattice had to be carefully optimised to reduce the orbit excursion, allowing the beams to fit inside a simple toroidal vacuum pipe that fits in the magnets. The table below gives the critical radii and clearances in this construction.

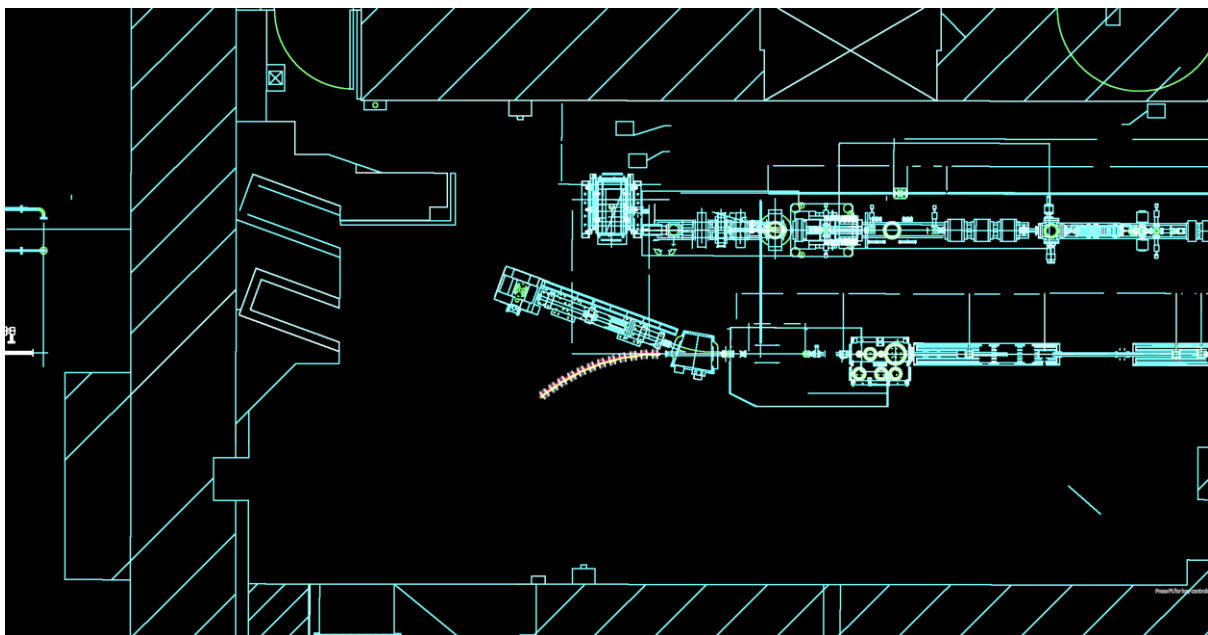
Object	Radius relative to magnet axis (mm)	Relative to vacuum pipe toroid (mm)	Difference (mm)
Beam centroids (widest spread in QF)	21.70	19.83	(NB: QF is displaced relative to pipe)
Vacuum pipe inner surface		23.75	3.92 outermost beam centroid to pipe
Vacuum pipe outer surface		25.40	1.65 pipe thickness
Shim holder inner surface (smallest in BD)	27.60	27.45	2.05 vacuum pipe to shim holder
Permanent magnet inner surface (smallest in BD)	30.70	30.55	3.10 thickest shim holder (BD)
Aluminium support inside	69.85		
Aluminium support outside	76.20		

The optimisation also displaced QF by 1.82mm outwards relative to the vacuum pipe. However, QF's inner radius is >7mm larger than BD's so this does not cause problems. There is a slight tension because the largest orbit excursions occur in QF but the smallest aperture is BD and this design tries to use a constant radius vacuum pipe to fit through both. The origin of this is historical because the

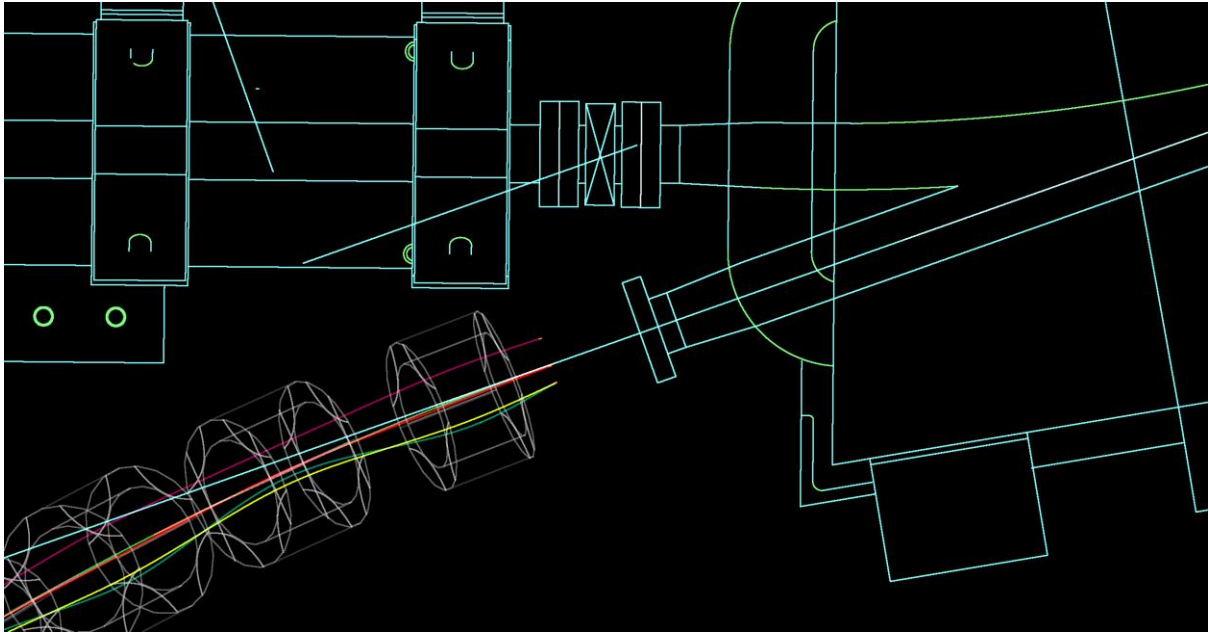
prototype magnets that were built corresponded to an earlier CBETA design where the vacuum pipe diameter varied to keep a roughly constant clearance from the beams.

The relatively short length of the beamline means all the magnets can be mounted to a single metal plate. Holes would be drilled at the coordinates required and the magnets affixed via 6-axis adjustable mounts for fine alignment. At the end of the beamline there needs to be a beam screen diagnostic that can detect the (x,y) position of the beam centroid to better than mm precision. To join the toroidal vacuum pipe to ATF (at the start) and the beam screen and beam stop (at the far end), there must be flanges on either end. One of these can be in place already when the pipe is threaded through the magnets, but the second has to be welded on afterwards.

The figure below shows the size of the proposed FFAG beamline in its probable location at ATF, with the beamline bending towards the west wall (bottom of drawing).



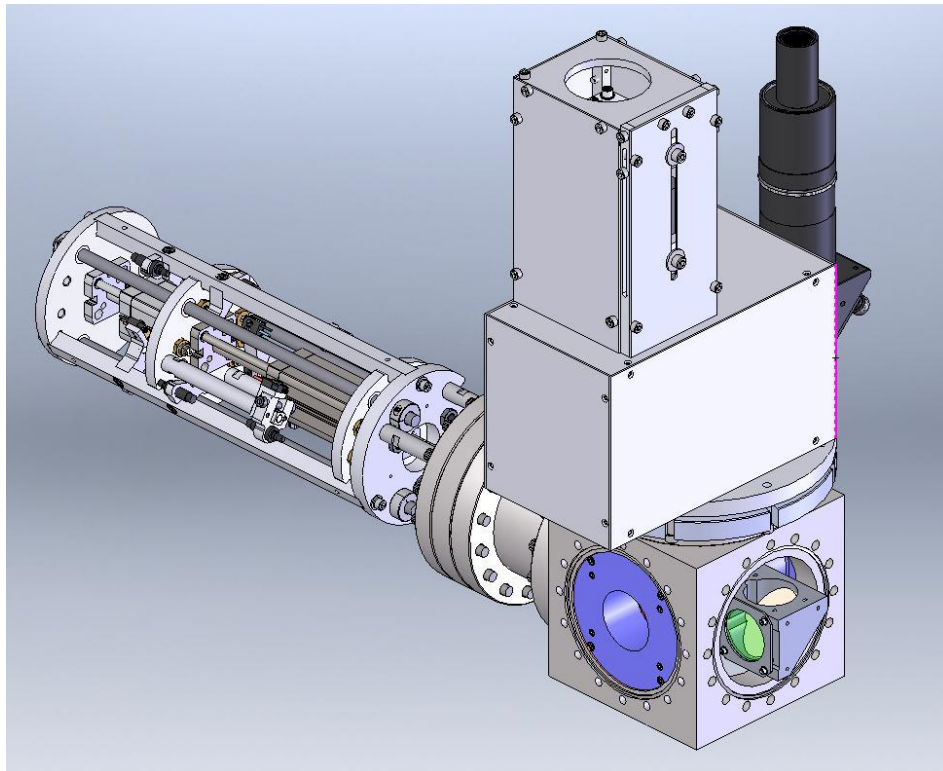
A zoomed in version (below) shows that the FFAG input orbits and angles are large compared to the ATF output pipe of this beam port. So it is probably necessary to make the table holding the FFAG able move sideways and rotate to put the output ATF beam down the nominal closed orbit for each energy. This requires a bellows on the vacuum connection and either manual or stepper motor movement. The 12 magnets only weigh 33kg in total so the mass of the table is not prohibitive.



2.4. Beam Screen Diagnostic

At the end of the beamline there will be a screen capable of detecting the (x,y) centroid of the beam or beam pulse. Desired accuracy is better than 0.5mm (preferably 0.1-0.2mm). The screen should be large enough to see the entire beam excursion: $\pm 20\text{mm}$ or more in X and $\pm 10\text{mm}$ or more in Y for vertical scanning. The screen may be a “destructive” diagnostic as it is the last element in the beamline. If the beam image is being picked up by a camera, it would improve accuracy to have a grid drawn on the screen for calibration.

A screen satisfying these criteria has been found within C-AD and is shown in the figure below.



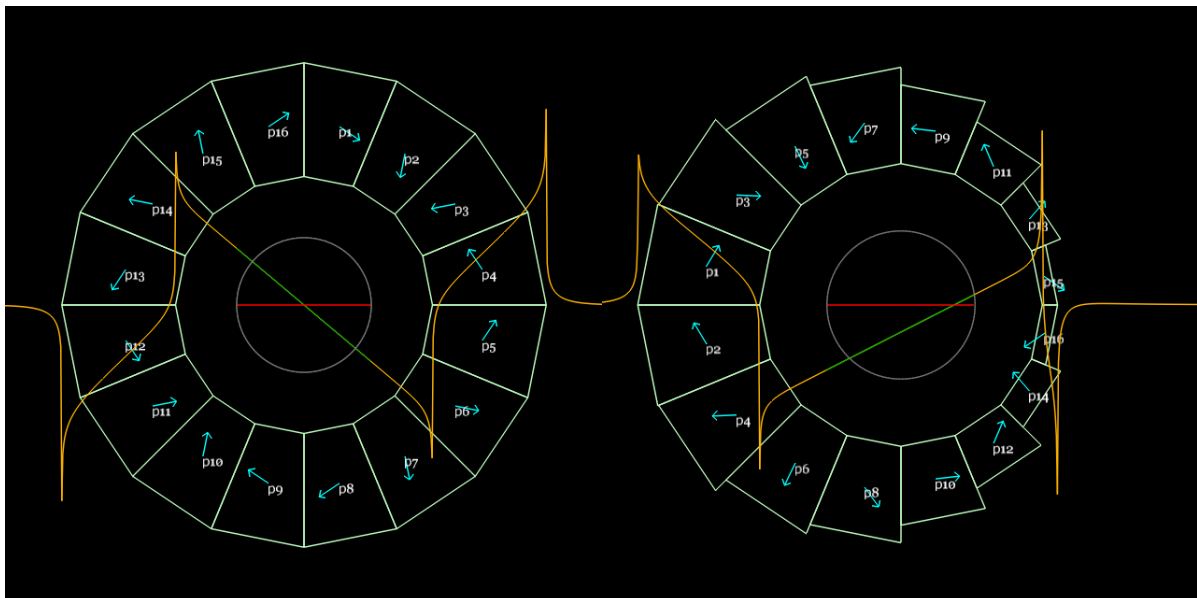
The cube (bottom right) is where the beamline flanges will be attached. It has a flange-to-flange distance of 6 inches. The arm for retracting the screen will not be operated for this experiment, as the screen is always the final element of the beamline, so being a destructive diagnostic is not a problem. While getting this diagnostic to work, it may be a good idea to temporarily attach it to the bellows at the beamline start (without the FFAG) so it can be tested on its own.

3. Halbach Permanent Magnets

All the materials for making the magnets have been already been purchased as part of CBETA R&D. As of 2016-Sep-28, several of the magnets have been constructed and shimmed, with the status of the 12 magnets shown in the table below.

QF1	BD1	Key:
QF2	BD2	
QF3	BD3	
QF4	BD4	
QF5	BD5	
QF6	BD6	
		Not yet constructed
		Awaiting rebuild
		Constructed
		Measured
		Shimmed

The figure below shows the design of the magnets in cross-section (QF on left, BD on right), with the calculated B_y field graphed across the horizontal aperture (orange and green lines). The blue arrows are the magnetisation direction of each block.



The magnets use the Neodymium-Iron-Boron grade N35SH from AllStar Magnetics and the current sheet simulation above uses an effective B_r of 1.194T (and $\mu_r=1$), which has proved a good fit to both OPERA-3D results and reality in terms of integrated field strength. The main parameters of these magnets are given in the table below.

Parameter	“QF” magnet	“BD” magnet	Units
Length	57.44	61.86	mm
Dipole $B_y(x=0)$	0	-0.37679	T
Quadrupole dB_y/dx	-23.624	19.119	T/m
Inner radius (magnet pieces)	37.20	30.70	mm
(shim holder)	34.70	27.60	mm
“Pole-tip” field (magnet pieces)	0.879	(-)0.964	T
Outer radius (magnet pieces)	62.45	59.43	mm
(tubular support)	76.2	76.2	mm

The magnet blocks are assembled into a 3D printed plastic mould, which in turn sits inside a section of aluminium tube for extra rigidity (see photographs below). Due to the arrangement of wedge shapes, the magnets are self-supporting like an arch and do not require support from the inside.

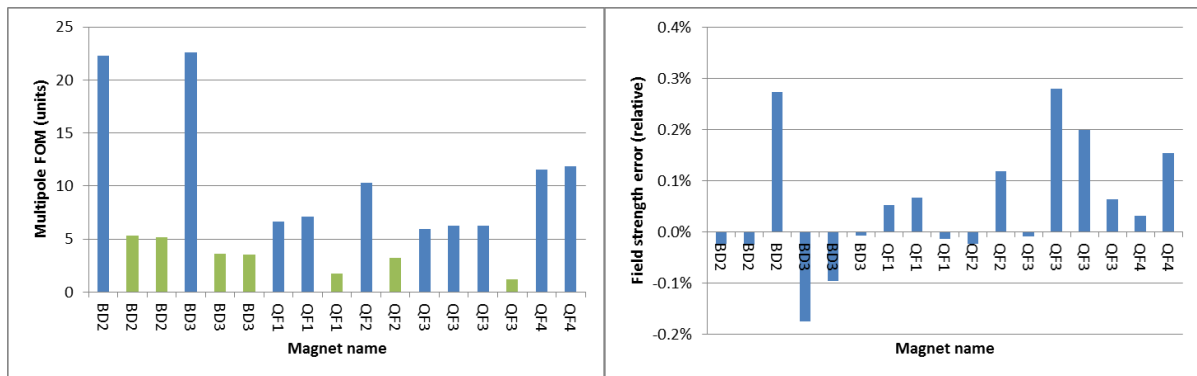


When the magnets have been measured once on one of the rotating coils at BNL, the harmonics found can be shimmed out by adding iron wires of various masses in a particular arrangement around the inner bore of the magnet. Each iron wire produces a field distortion looking like an external dipole and the sum of these is calculated to cancel the harmonics. The iron wires are held in the correct positions by a 3D printed shim holder, shown in the photograph below. The magnetic force pulling the shims towards the permanent magnet pieces also helps hold them in place in most cases, although an additional thin plastic film can be added to the inside to prevent damage. The

photograph below shows the shim holder taped into the magnet, although now the process is confirmed to work, it can be glued there permanently.



The graphs below show the field quality (left) and field strength error (right) of all measurements on these magnets so far. Green bars are shimmed magnets. The “Multipole FOM” is the square root of the sum of squares of all multipole harmonics measured at R=10mm in units (10^{-4} of the main pole).



Values reported for the shimmed QF magnets correspond to $(0.64 \text{ to } 1.02) \times 10^{-3}$ maximum relative field error from higher harmonics across the whole range of the beams. The shimmed BD magnets produce the value $(2.7 \text{ to } 5.2) \times 10^{-3}$, although the coil used for these was only 12.4mm radius, making the extrapolation out to the full 17.8mm beam excursion unreliable (the R=10mm multipole values are always valid). Second shim iterations are possible if a shimmed magnet is not good enough: this has worked in the past and may be used on the BD magnets.

The magnets also have a temperature coefficient of approximately $-0.12\%/K$, which is manifested as a change of B_r , i.e. the overall strength of the magnet. Thus, the variability seen in the strength error graph corresponds to a 2-3K temperature shift. This effect is not expected to be a problem for the short ATF FFAG beamline, since even a large 10K temperature swing would be equivalent to changing the beam energy by 1.2% (e.g. from 79 to 80MeV), a sub-mm change in orbit location.

Examples of the multipole errors measured with the rotating coil after one iteration of shimming are given in the table below, for R=10mm. The worst case (BD2) is on the left and the best case (QF3) on the right.

Field harmonic	Normal units	Skew units	Field harmonic	Normal units	Skew units
Dipole	-19653.83	-0.00	Dipole	0.00	-0.00
Quadrupole	10000.00	0.00	Quadrupole	10000.00	0.00
Sextupole	0.83	-0.99	Sextupole	-0.18	-0.94
Octupole	-3.98	2.38	Octupole	0.34	0.17
Decapole	1.68	-0.90	Decapole	-0.65	0.09
Dodecapole	-0.08	-0.09	Dodecapole	-0.05	0.02
14-pole	-0.03	-0.06	14-pole	-0.02	-0.01
16-pole	0.03	-0.03	16-pole	-0.00	0.00
18-pole	0.01	-0.02	18-pole	0.00	0.00
20-pole	0.00	0.01	20-pole	-0.00	-0.00
22-pole	0.00	0.00	22-pole	-0.00	-0.00
24-pole	0.00	-0.00	24-pole	-0.00	0.00
26-pole	-0.00	-0.00	26-pole	0.00	-0.00
28-pole	0.00	0.00	28-pole	0.00	-0.00
30-pole	-0.00	-0.00	30-pole	-0.00	-0.00

4. Requirements from ATF

An outline of the experimental requirements are given below.

4.1. Beam Energy and Intensity

Ideally the whole range 20-80MeV scannable in small steps (say 5MeV). The most important figure is the ratio between the top and bottom energies, so for instance the range 20-30MeV is much more valuable (a factor of 1.5) than the range 70-80MeV (a factor of 1.14).

The beam only needs to be intense enough to give a good reading of the beam centroid position on the screen at the end of the beamline, so high average currents or bunch charges are not required.

4.2. Other Beam Parameters, Steering and Scanning

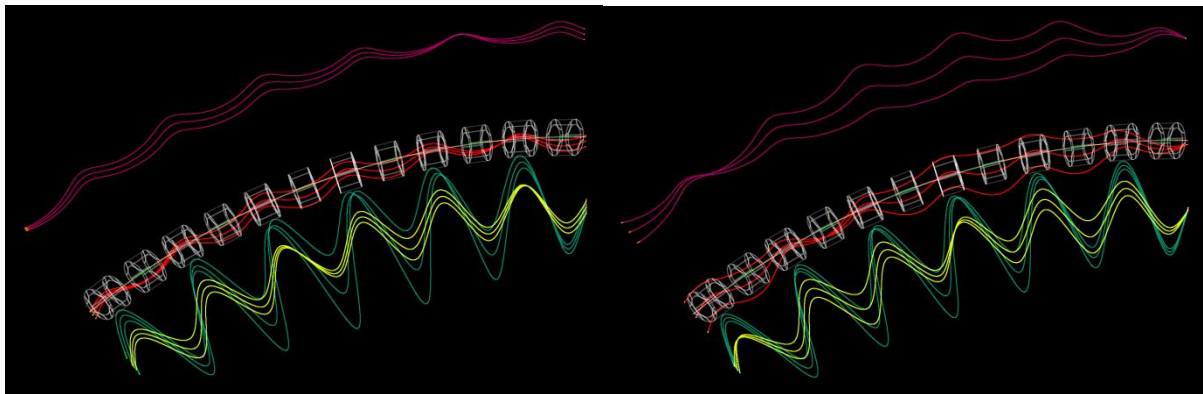
The matching plane for the cell is defined to be half way through the D2 drift, that is, 32.45mm along the vacuum pipe's circle before the first magnet (QF). Periodic matching conditions at this point of the cell can be determined from the Muon1 code but extra care needs to be taken on the first cell (the input plane for the beamline), since the fringe fields overlap and the first cell only has fringe field from one side. Tracking backwards allows correct "closed orbit" positions at the start of the first cell to be calculated, as well as positions at the end of the last cell: these and the periodic orbit positions are shown in the table below. The largest difference between periodic and entrance coordinates is found in the angle ($\sim 8\text{mrad}$) at the lowest energy.

Beam Energy	Entrance x (mm)	Entrance x' (rad)	Periodic x (mm)	Periodic x' (rad)	Exit x (mm)	Exit x' (rad)
20MeV	-11.99	-0.19425	-12.09	-0.18617	-12.13	-0.18914
40MeV	-12.41	-0.09679	-12.46	-0.09285	-12.48	-0.09450

60MeV	-0.74	-0.02802	-0.77	-0.02616	-0.77	-0.02614
80MeV	18.48	0.02436	18.48	0.02440	18.50	0.02559

As mentioned in section 2, the large input angles and offsets might be difficult to produce from the ATF beam port given the long narrow beam pipe it comes out of, so another option is to allow the table with the FFAG on it to shift and rotate for each energy so that the beam coming from the centre of the ATF output pipe goes into the expected closed orbit. Then ATF would only have to produce small changes to the offsets and angles around this orbit.

The figures below show the effect of varying the entrance position by $\pm 1\text{mm}$ (left) and the entrance angle by $\pm 10\text{mrad}$ (right). Trajectories have been magnified transversely by 16x for visibility.



It is hoped to do a scan in entrance angle and position around the closed orbit position for each energy tested. Step sizes might be 0.5mm and 5mrad, for example, with the range being largest for the middle energies, since the outer energies will tend to hit the beam pipe. A “large” scan range here would be 10 steps in either direction. Still, it may be possible to do a large scan of the outer energies and just record when the beam was not transmitted. A scan in the vertical phase space plane (y, y') is also of interest if the steering magnets permit. In all cases, the output (x, y) centroid position would be recorded for each energy and injection setting.

Matched optical functions at the matching plane are given below. As this study only looks at the beam centroid position, it is not necessary to match these functions, as the centroid will behave the same way in any case. However keeping the beam’s optical functions of the same order of magnitude as the matched ones will prevent the beam becoming excessively spread out.

Beam Energy	β_x (m)	α_x	β_y (m)	α_y
20MeV	0.2583	-3.9992	0.1905	2.3516
40MeV	0.2429	-1.2540	0.3409	1.6601
60MeV	0.3489	-1.1027	0.7365	2.2325
80MeV	0.4122	-0.9987	1.2793	2.8975

4.3. Controls

It would be helpful if the image picked up by the beam screen camera could be seen directly in the control room, which requires some interfacing of the camera to the ATF control system. A fallback solution would be to save the photos to a network disk. The processing of the image can be done either with existing software for determining beam centroids from images, or if this is not available for some reason, Stephen Brooks can write code that converts the images to bitmaps and finds the average position of the brightest pixels.

Good data will be obtained if the “scans” of position and angle can be done over relatively large arrays, say 20x20 readings in (x,x') phase space. This would suggest using scripting to loop over these parameters in the control software, then calculating and applying the magnet settings required for each pulse. Alternatively the tables of settings could be pre-calculated and entered by hand, but this would be laborious and more likely to introduce errors.

4.4. Schedule

It has been suggested that the FFAG beamline and supporting table be installed during an anticipated shutdown of ATF around New Year 2017, although the exact date has not been fixed yet.

Sessions with beam will require around a thousand individually-measured pulses, which scan in x, x' (and possibly y, y'). Changes in energy will probably be the least frequent. Energy changes may be accompanied by a tunnel access to move the FFAG table so that injection for the new energy is lined up with the ATF output, as well as re-tuning of ATF's linac and other systems to provide the new energy. If tunnel access is not possible for radiation or other operational reasons, a table with motion controllers (two stepper motors) can be designed.

The experiment will probably need up to ~3 weeks of work, separated into two or three sessions separated a few weeks to months. The experimenters are at BNL so can probably adjust their schedule as needed. For example, the first session could concentrate on getting the systems working and beam through the channel, the second could do the main scan measurements and the third will refine the scans on the basis of previous measurements, plus push towards the far ends of the energy range, which will be more challenging.

5. List of Work Items

The table below attempts to list the main tasks that need to be done for this experiment and suggests staff or groups who could help with each one.

Area	Task	Staff
Simulation	Verify tracking with fieldmaps, generate survey coordinates	Stephen Brooks
	Generate OPERA-3D fieldmaps	Nick Tsoupas
Magnets	Build remaining magnets	Stephen Brooks, George Mahler
	Shim and remeasure magnets	Stephen Brooks, John Cintorino
	Survey to find magnetic centres	SMD (John Cintorino, Peter Wanderer)
Girder/table	Design and generate drawings	Lead by George Mahler
	Build table of correct height	“

	Drill holes in table to affix magnets	“
	Install magnet mounts	“
	Install magnets in approximate positions in mounts	“
Vacuum pipe	Bend an aluminium pipe to be toroidal with the required radius of curvature	“
	Thread pipe through magnets	“
	Weld required flanges to either end of pipe	Vacuum group?
Diagnostics	Get beam screen and beam stop/end-plate and attach to far end of vacuum pipe	Diagnostics group, to be consulted
	Prepare read-out electronics and computer software	“
Installation	Transport table including magnets in approximate positions and vacuum pipe to ATF hall and fix to floor	Technicians
	Join entrance flange to end of existing ATF beamline	ATF (or C-AD) technicians
	Connect diagnostics to read-out electronics	Diagnostics group
	Install beam stop and modify shielding as required	ATF (or C-AD) technicians
Final alignment	Determine alignment relative to final part of ATF beamline, or ATF's beam coordinate system	Alignment group
	Align magnets using the mounts to put magnetic centres in correct locations	Alignment group with input from Stephen Brooks
Beam time sessions	Demonstrate beam transport and scan in phase space	Mikhail Fedurin, ATF staff, with supervision from Stephen Brooks, Dejan Trbojevic
Data processing	Convert beam screen images into beam centroids and determine optical parameters	Stephen Brooks with help from diagnostics group
Uninstallation	Disconnect and remove table if/when this is necessary	ATF (or C-AD) technicians